Electronic Supplementary Material (ESI) for Journal of Materials Chemistry A
This journal is © The Royal Society of Chemistry 2018

Supporting Information

Precise nanopore tuning for high-throughput desalination membrane via codepostion of dopamine and multifunctional POSS

Xinda You[a,b], Hong Wu[a,b,c] *, Yanlei Su[a,b], Jinqiu Yuan[a,b], Runnan Zhang[a,b], Qianqian Yu[a,b], Mengyuan Wu[a,b], Zhongyi Jiang[a,b] * and Xingzhong Cao[d]

[a] *Key Laboratory for Green Chemical Technology, School of Chemical Engineering and Technology, Tianjin University, Tianjin 300072, China*

[b] *Collaborative Innovation Center of Chemical Science and Engineering (Tianjin), Tianjin, 300072, China*

[c] *Tianjin Key Laboratory of Membrane Science and Desalination Technology, Tianjin University, Tianjin 300072, China*

[d] *Key Laboratory of Nuclear Analysis Techniques, Institute of High Energy Physics, Chinese Academy of Sciences, Beijing 100049, China*

* *E-mail: wuhong@tju.edu.cn Tel: 86-22-23500086 Fax: 86-22-23500086*

* *E-mail: zhyjiang@tju.edu.cn Tel: 86-22-23500086 Fax: 86-22-23500086*

2. Experimental section

2.1 Preparation of POSS-PDA/PAN membranes

Firstly, the membrane-forming solution was prepared by dissolving 40 mg of dopamine hydrochloride and varied content of $8NH_3Cl$-POSS in Tris-HCl buffer solution (20ml, 50 mM, pH=8.5). The dopamine hydrochloride and $8NH_3Cl$-POSS would transform into dopamine and $8NH_2$-POSS in alkali solution, respectively (Fig. S1). Secondly, for deposition, circle pieces of PAN substrates (area of 13.4 cm^2) were submerged in the abovementioned solution followed by oscillation for a schedule time (150 r/min). Finally, the membranes were rinsed in DI water for 20 min to remove unreacted residuals and cured at 60 °C in a vacuum oven for 10 min. All of the as-fabricated membranes were stored in DI water before testing.

Table S1. The specific fabrication parameters for all the membranes tested in this work.

Membrane name	$8NH_3Cl$-POSS content (mg)	Dopamine hydrochloride content (mg)	Deposition time (min)	Washing time (min)	Curing temperature (°C)	Curing time (min)
PAN substrate	0	40	0	20	60	10
POSS(0)/PDA(75)	0	40	90	20	60	10
POSS(5)/PDA(75)	5	40	75	20	60	10
POSS(8)/PDA(75)	8	40	75	20	60	10
POSS(10)/PDA(75)	10	40	75	20	60	10
POSS(12)/PDA(75)	12	40	75	20	60	10
POSS(16)/PDA(75)	16	40	75	20	60	10
POSS(12)/PDA(60)	12	40	60	20	60	10
POSS(12)/PDA(90)	12	40	90	20	60	10
POSS(12)/PDA(105)	12	40	105	20	60	10
POSS(12)/PDA(120)	12	40	120	20	60	10

Table S1 summarized the specific fabrication parameters for all the membranes tested in this work. For convenient narration, the fabricated membranes were designated as POSS(***x***)/PDA(***y***) where ***x*** represented the content of $8NH_3Cl$-POSS in membrane-forming solution and ***y*** represented the deposition time. For example, POSS(12)/PDA(75) was the membrane with $8NH_3Cl$-POSS of 12 mg in membrane-forming solution and deposition time of 75 min. Here, the ***x*** ranged from 0 to 16 and the ***y*** ranged from 60 to 120.

2.2 Preparation of POSS-PDA nanoaggreagates

The POSS-PDA nanoaggregates formed in solution were collected for investigating membrane-forming mechanism. The content of $8NH_3Cl$-POSS was fixed at 12 mg and the deposition time ranged from 30 to 75 min (oscillating at 150 r/min). To purify the melanin-like nanoaggregates, the resultant solution was centrifuged (11000 r/min) for 30 min and rinsed with DI water by ultrasonic (100 kHz, 10 min) for three cycles. Finally, the dispersive nanoparticles were collected by centrifuge (11000 r/min) for 30 min and overnight lyophilization.

2.3 Membrane characterization

The membrane samples were freeze-dried for 24h before characterization.

Fourier transform infrared spectroscopy. The experiments were run with air as the background. The membrane/nanoparticle samples were dried in vacuum oven at 40 °C for 12 h before characterization.

X-ray photoelectron spectroscopy. The takeoff angle of photoelectron for XPS instrument was set at 90° (the measured depth near 10 nm) and the survey spectra were 0-1100 eV.

Water contact angles. The interval between drop and measurement was 10~20 s.

Zeta potential. First, the samples were immersed in 0.001 mol/L KCl solution (pH=6±0.2) for 12 h before measurement. Then, the samples were clipping into pieces (1 cm×0.5 cm), which were fixed to the mould of the equipment. The zeta potential of samples was measured utilizing 0.001 mol/L KCl solution (pH=6±0.2) at 25±0.5 °C and each sample was measured for 4 times to eliminate error.

Pore size and pore size distribution measurement. The concentrations of permeate and feed solutions were determined by a chemical oxygen demand analyzer (COD, Leichi COD-571, China). The Stokes radii of PEG was calculated based on their average Mw by followed Eq. (2),

$$r = 16.73 \times 10^{-12} \times M_w^{0.557} \tag{2}$$

where r (m) was the Stokes radii of PEG and M_w was the average molecular weight (Da). Subsequently, we related obtained solute rejection with the Stokes radii and transformed it into a correlation function. Finally, the pore size distribution was described by the following probability density function namely Eq. (3),

$$\frac{\mathrm{d}R\left(d_p\right)}{\mathrm{d}d_p} = \frac{1}{d_p \ln \sigma_p \sqrt{2\pi}} \exp\left(-\frac{\left(\ln d_p - \ln \mu_p\right)^2}{2\left(\ln \sigma_p\right)^2}\right) \tag{3}$$

where μ_p was defined as the geometric mean diameter of solute at 50% solute rejection, σ_p was defined as the ratio of the solute radius when solute rejections were 84.13% and 50%, representing the geometric standard deviation of μ_p.

3. Result and disccusion section

3.1 Formation mechanism of POSS-PDA/PAN membranes

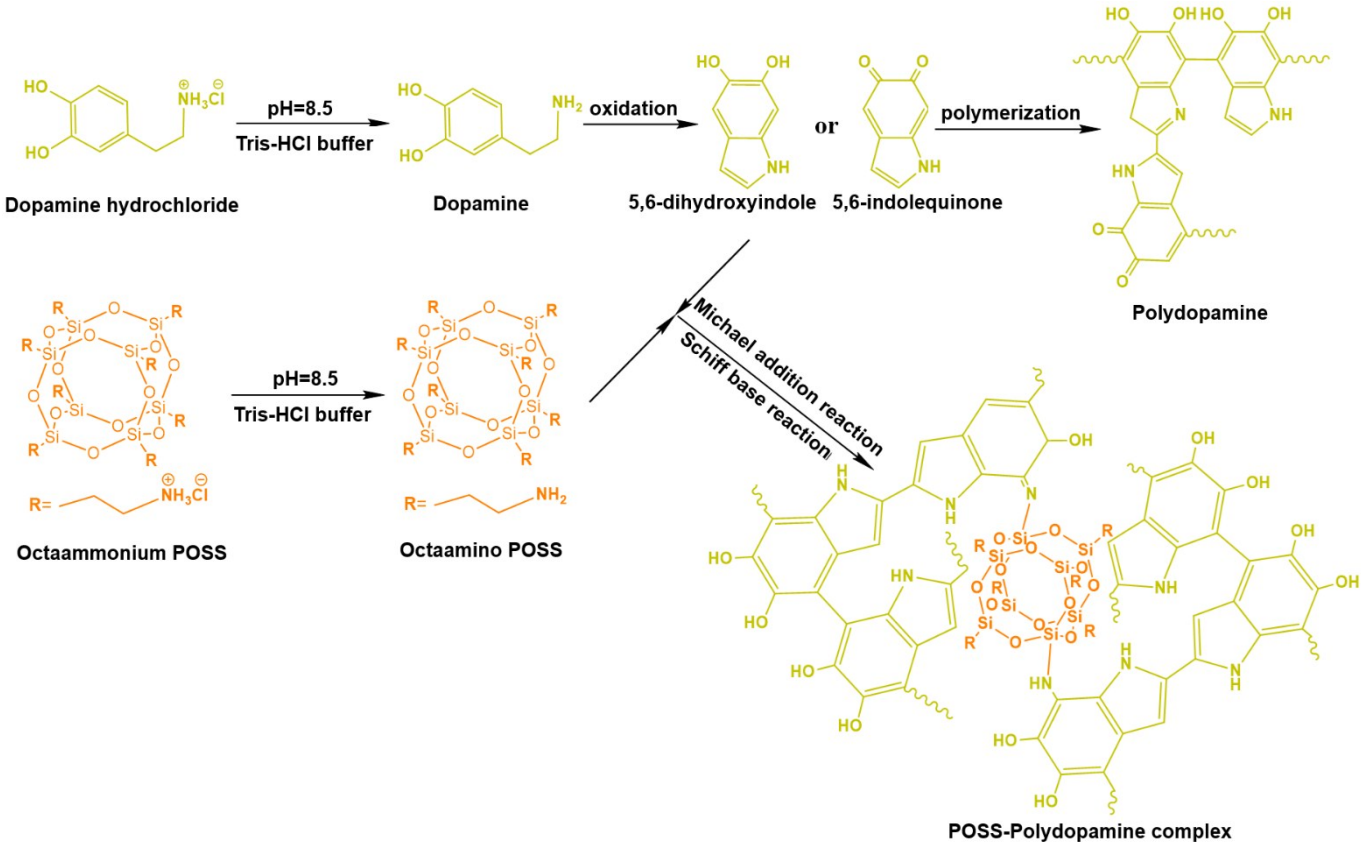

Fig.S1. The probable reaction routes in this work

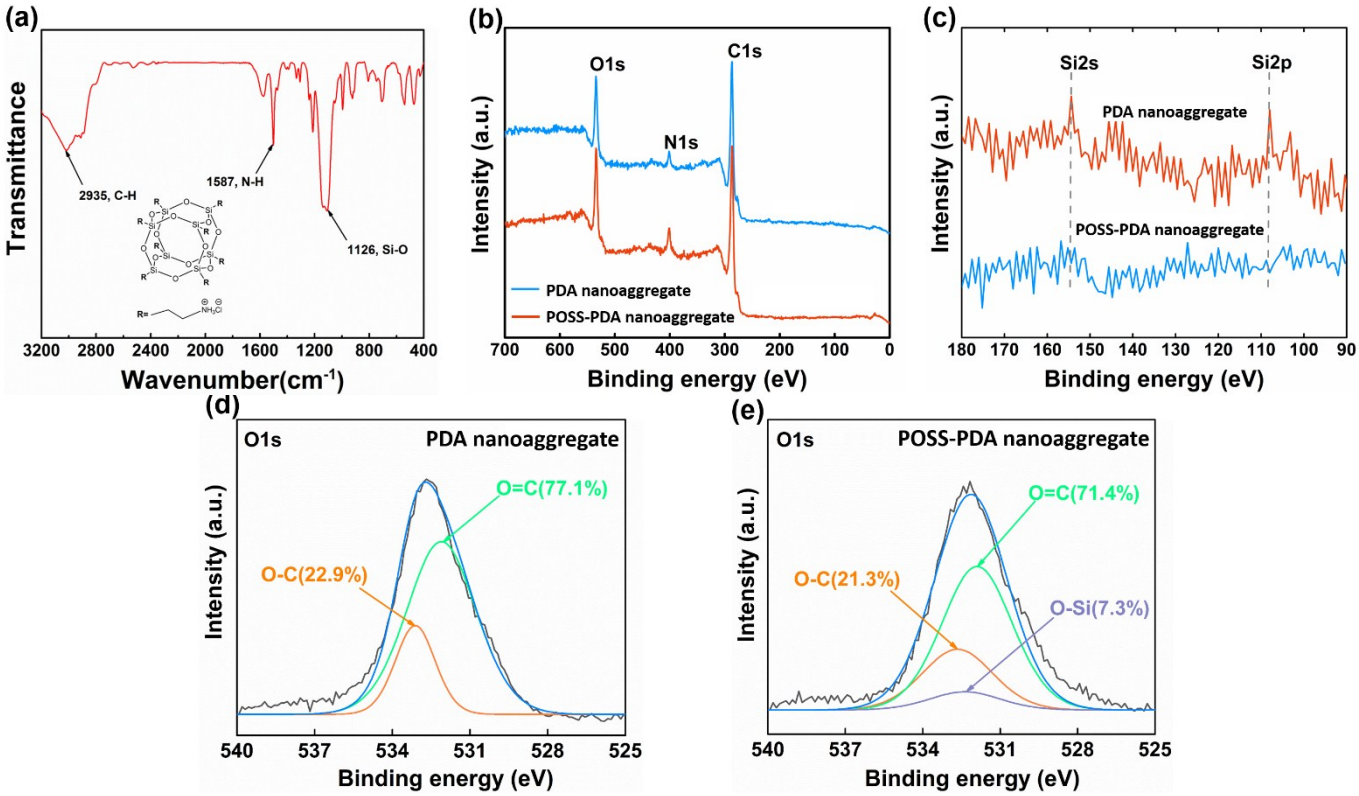

Fig. S2. (a) The FTIR spectra of 8NH_3Cl-POSS; (b) and (c) The XPS results of PDA and POSS-PDA nanoaggregates; (d) and (e) the high-resolution XPS of O1s peak for PDA and POSS-PDA nanoaggregates (O-C: 533.3 eV, O=C: 531.2 eV, O-Si: 532.3 eV). (The deposition time was 75 min and the 8NH_3Cl-POSS content in solution was 12 mg)

Table S2. The EDX result of POSS-PDA nanoaggregates with different deposition time.

Powder code	8NH_3Cl-POSS content (mg)	Deposition time (min)	C (%)	O (%)	N (%)	Si (%)
1#	12	10	57.7	27.5	14.4	0.4
2#	12	20	58.2	25.5	15.5	0.8
3#	12	30	65.3	20.7	13	1.0
4#	12	75	66.0	18.5	14.0	1.5

Table S2 summarized the elementary composition of POSS-PDA nanoaggregates with different deposition time.

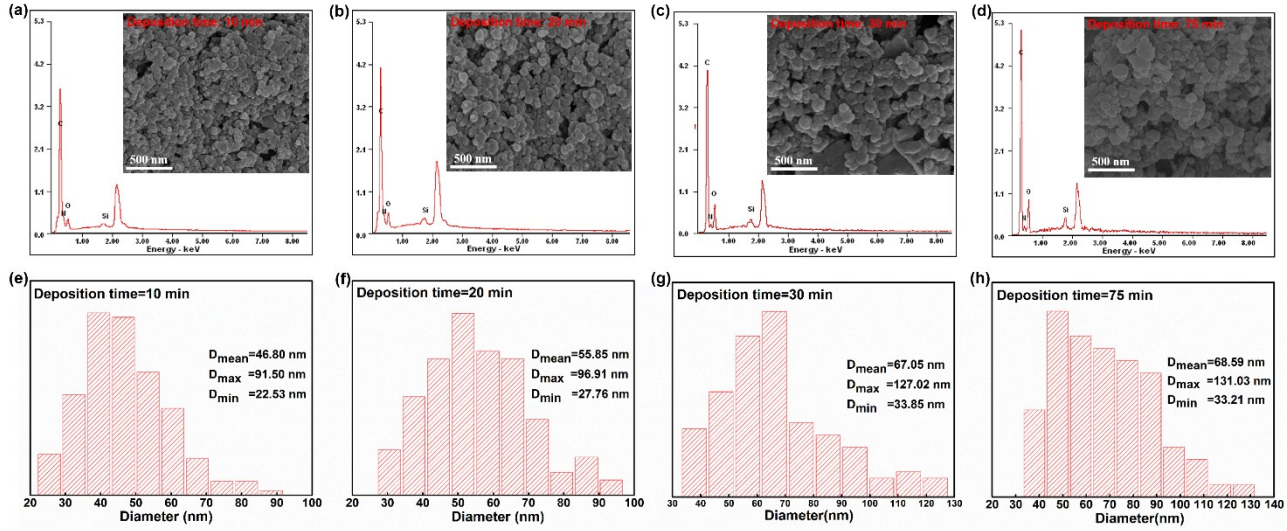

Fig. S3. (a-d) The SEM images and energy dispersive spectrum of POSS-PDA nanoaggregates with different deposition time; (e-g) the particles size distribution of POSS-PDA nanoaggregates with different deposition time (calculated by image analysis software based on SEM images).

3.2 Characterization of POSS-PDA/PAN membranes

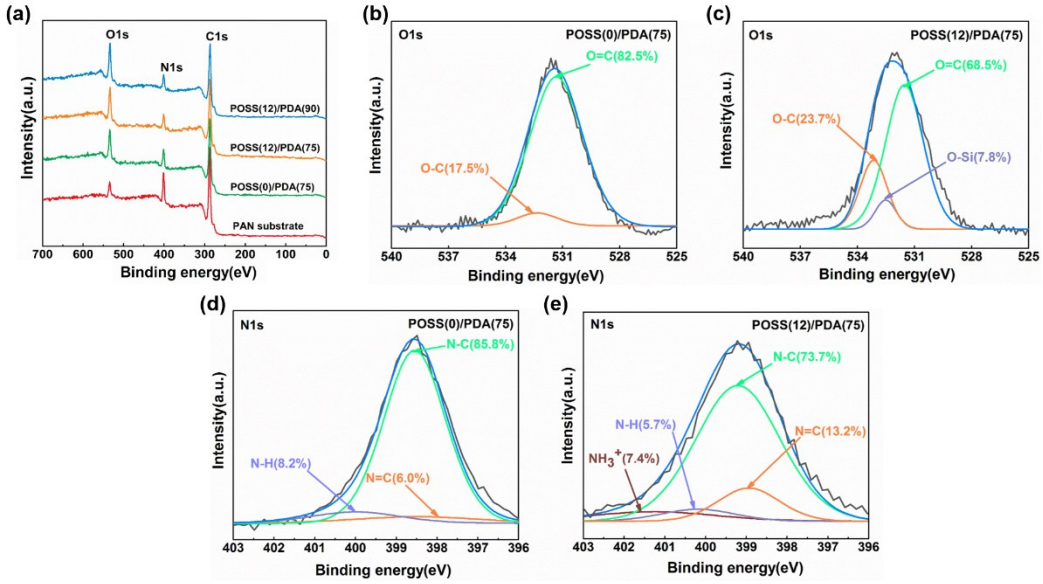

Fig. S4. (a) The XPS result of membranes; (b-c) the high-resolution XPS of O1s peak for POSS(0)/PDA(75) and POSS(12)/PDA(75); (d-e) the high-resolution XPS of N1s peak for POSS(0)/PDA(75) and POSS(12)/PDA(75). (O-C: 533.3 eV, O=C: 531.2 eV, O-Si: 532.3 eV, N-C: 399.5 eV, N=C: 398.9 eV, N-H: 400.2 eV, NH_3^+: 401.5 eV)

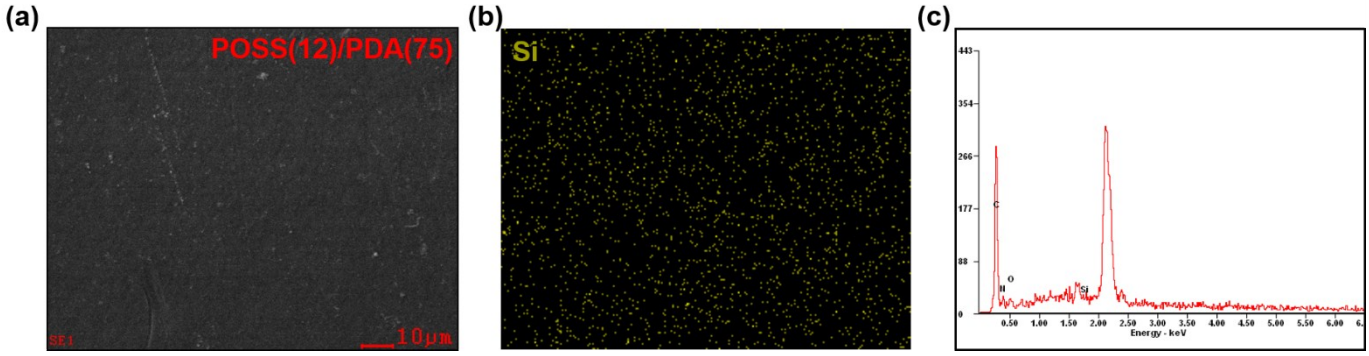

Fig. S5. (a) The SEM image for EDX mapping, (b) EDX Si mapping and (c) EDX result of POSS(12)/PDA(75) membrane.

Table S3. The measured water contact angles (θ), roughness area ratio (r), corrected water contact angles (θ^*) and surface roughness of the membranes.

Membrane name	θ[a](°)	surface area[b] (μm²)	Projected area[c] (μm²)	r[d]	θ^*[e] (°)	Roughness[f] (nm)
PAN substrate	49.6±0.1	4.07	4.0	1.018	50.5±0.2	6.4
POSS(0)/PDA(75)	52.6±0.2	4.12	4.0	1.030	53.5±0.3	7.3
POSS(5)/PDA(75)	51.6±0.2	4.26	4.0	1.065	54.3±0.3	11.5
POSS(8)/PDA(75)	54.6±0.2	4.19	4.0	1.048	56.4±0.3	12.4
POSS(10)/PDA(75)	56.3±0.2	4.28	4.0	1.070	58.8±0.3	13.3
POSS(12)/PDA(75)	55.5±0.1	4.29	4.0	1.073	58.5±0.2	13.8
POSS(16)/PDA(75)	58.1±0.2	4.83	4.0	1.208	64.1±0.4	17.3
POSS(12)/PDA(60)	53.4±0.2	4.16	4.0	1.04	55.0±0.3	10.8
POSS(12)/PDA(90)	56.7±0.1	4.36	4.0	1.090	59.8±0.2	15.0
POSS(12)/PDA(105)	56.9±0.2	4.41	4.0	1.103	60.3±0.3	17.6
POSS(12)/PDA(120)	57.3±0.2	4.68	4.0	1.170	62.5±0.3	19.4

[a] Contact angle goniometer was used to measure sessile drop contact angles of DI water on the air-dried membrane samples and four locations

of each sample were measured to eliminate error; the interval between drop and measurement was 5 s.

[b] The effect surface area of membranes obtained from AFM characterization.

[c] The vertical projection surface area of membranes obtained from AFM characterization.

[d] The roughness area ratio was equal to the ratio of surface area and project area.

[e] Corrected water contact angle calculated by $\cos\theta^{*}=\cos\theta/r$.

[f] Root-mean-square surface roughness obtained from AFM characterization.

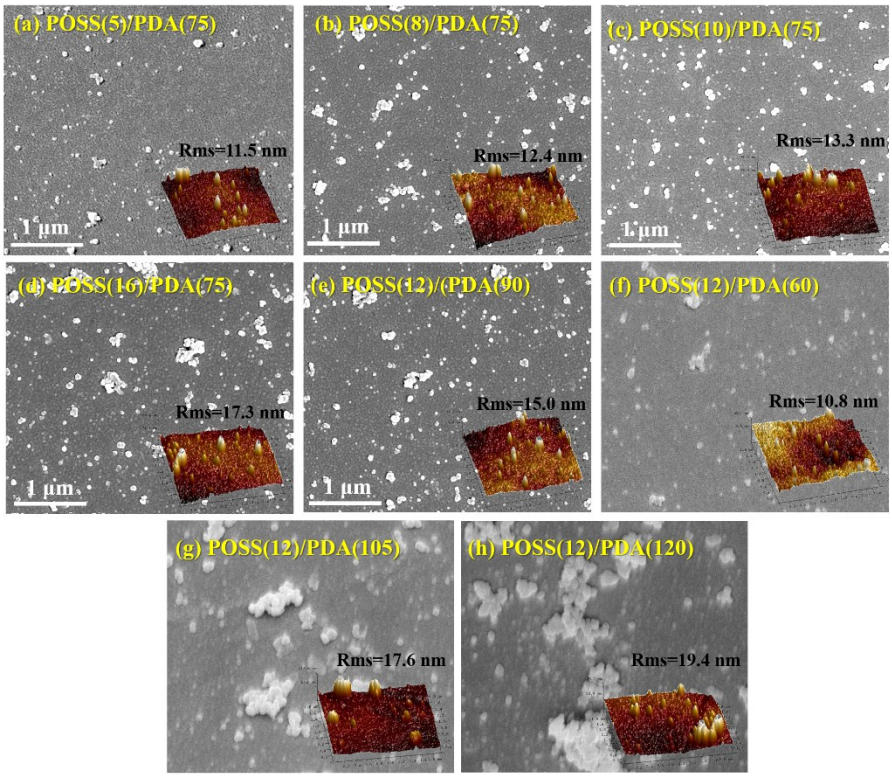

Fig. S6. The surface morphology of membranes with different deposition time and different 8NH_3Cl-POSS content in membrane-forming solution.

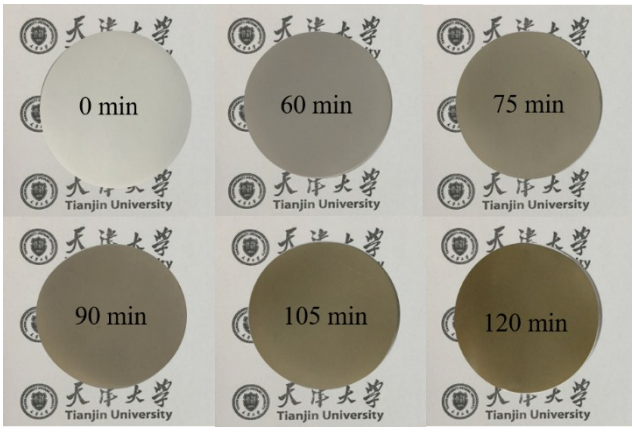

Fig. S7. The digital photographs of membranes with different deposition time (The content of 8NH_3Cl-POSS in membrane-forming solution was 12 mg).

Table S4. The summary of zeta potential of the membranes.

Membrane name	Zeta potential (mV)
PAN substrate	-65.94±0.4
POSS(0)/PDA(75)	-57.71±0.3
POSS(5)/PDA(75)	-56.86±0.3
POSS(8)/PDA(75)	-54.8±0.4
POSS(10)/PDA(75)	-52.57±0.2
POSS(12)/PDA(75)	-50.00±0.4

POSS(16)/PDA(75)	-47.27±0.3
POSS(12)/PDA(60)	-46.42±0.3
POSS(12)/PDA(90)	-51.49±0.3
POSS(12)/PDA(105)	-52.04±0.3
POSS(12)/PDA(120)	-54.34±0.4

The zeta potential was measured utilizing 0.001 mol/L KCl solution (pH=6.0±0.2) at 25±0.5 °C and each sample was measured for 4 times to eliminate error. The summary of zeta potential for all the samples was list in Table S4. Each above value was based on the average of two independent membranes fabricated under the same condition.

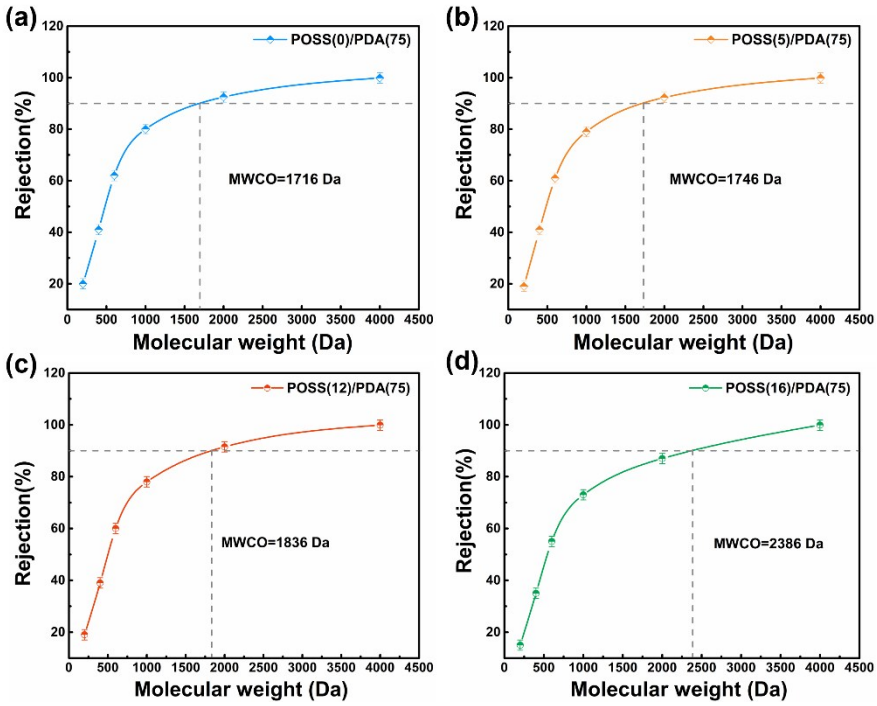

Fig. S8. The molecular weight cut-off of membranes with different 8NH_3Cl-POSS content in membrane-forming solution. (Deposition time was fixed at 75 min)

3.3 Separation performance of membranes

Table S5. The summary of separation performance of all the membranes tested in this work.

Membrane name	Pure water flux (L m^{-2} h^{-1})	Permeance (L m^{-2} h^{-1} MPa^{-1})	Orange GII rejection (%)	Methyl blue rejection (%)	Congo red rejection (%)	Alcian blue rejection (%)
PAN substrate	261.7±2	2617±20	39.2±2	63.9±2	74.3±2	58.0±2
POSS(0)/PDA(75)	79.2±2	792±20	91.1±2	93.4±2	98.2±2	93.6±2
POSS(5)/PDA(75)	86.8±1	868±10	90.7±2	93.6±1	98.1±1	93.8±1
POSS(8)/PDA(75)	94.2±1	942±10	90.6±1	93.8±1	98.0±2	93.5±1
POSS(10)/PDA(75)	99.1±1	991±10	90.6±2	93.7±1	98.1±1	93.8±2
POSS(12)/PDA(75)	109.9±1	1099±10	90.5±1	93.6±1	98.0±1	93.9±1
POSS(16)/PDA(75)	123.7±2	1237±20	74.6±2	92.5±2	97.9±1	93.0±1
POSS(12)/PDA(60)	151.7±2	1517±20	80.2±1	86.1±1	97.8±1	90.6±1
POSS(12)/PDA(90)	76.6±3	766±30	88.2±2	92.7±1	98.0±2	93.9±2
POSS(12)/PDA(105)	64.5±1	645±10	91.0±2	96.1±2	98.1±2	95.1±1
POSS(12)/PDA(120)	23.6±1	236±10	93.1±2	96.8±2	98.8±2	95.3±2

Table S5 summarized the pure water flux and dye rejection of all the membranes tested in this work. (Testing condition: 100 ppm dye feed under 0.1 MPa; 25 °C; 13.4 cm^2 membrane area; each above value was based on the average of two independent membranes fabricated under the same condition).

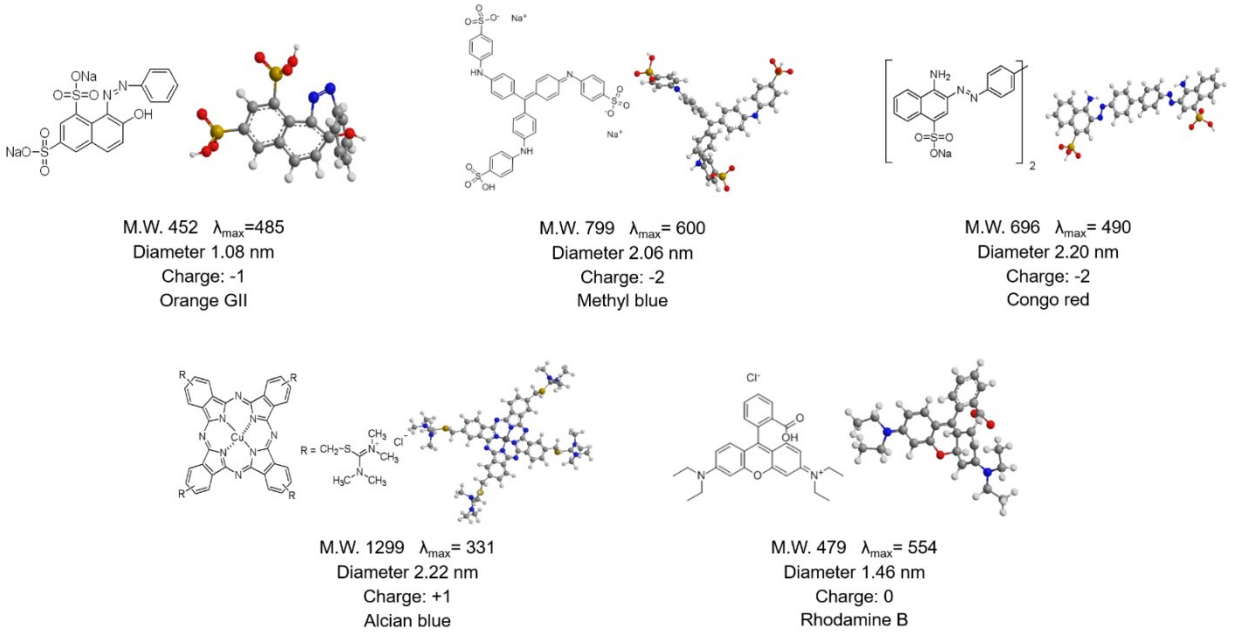

Fig. S9. The characteristics of organic dyes used in this work (Notes: M.W.=molecular weight; λ_{max}=maximum absorption wavelength). (The minimized-energy conformation of organic dyes was estimated using a Molecular Mechanism 2 method in Chem3D[1])

Table S6. The summary of permeation flux (J) during dye removal process of all the membranes tested in this work.

Membrane name	$J_{\text{Orange GII}}$ (L m^{-2} h^{-1})	$J_{\text{Methyl blue}}$ (L m^{-2} h^{-1})	$J_{\text{Congo red}}$ (L m^{-2} h^{-1})	$J_{\text{Alcian blue}}$ (L m^{-2} h^{-1})
PAN substrate	216.3±1	213.6±2	213.7±2	213.6±2
POSS(0)/PDA(75)	73.4±2	74.3±2	75.6±2	75.6±2
POSS(5)/PDA(75)	78.1±1	79.9±1	78.8±2	80.6±1
POSS(8)/PDA(75)	86.8±1	82.6±1	81.3±2	83.9±1
POSS(10)/PDA(75)	91.2±1	85.3±2	84.6±1	87.1±2
POSS(12)/PDA(75)	97.7±1	107.0±1	98.3±1	101.9±1
POSS(16)/PDA(75)	113.6±1	119.5±1	114.6±2	115.1±1
POSS(12)/PDA(60)	130.4±1	142.4±1	130.0±1	141.5±1
POSS(12)/PDA(90)	66.7±2	77.9±1	74.1±2	77.0±2
POSS(12)/PDA(105)	46.7±2	52.5±2	53.4±2	53.4±1
POSS(12)/PDA(120)	21.4±2	22.7±2	23.1±2	23.6±2

Table S6 summarized the permeation flux (J) during the dye removal process of all membranes, which was relatively significant in practical application. (Testing condition: 100 ppm dye feed under 0.1 MPa; 25 °C; 13.4 cm^2 membrane area; each above value was based on the average of two independent membranes fabricated under the same condition.)

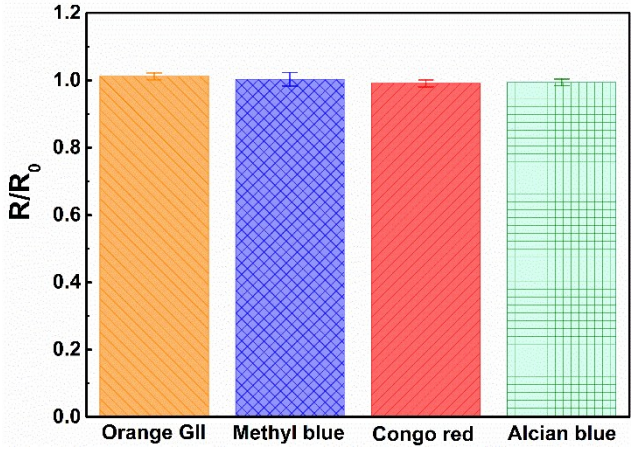

Fig. S10. The effect of adsorption on dye rejection for POSS(12)/PDA(75).

The absorption of organic dyes on membranes would probably lead to unreal rejection value for separation performance. To exclude the effect of dye adsorption, we performed pre-filtration experiment by using high-concentration organic dye feed (200 ppm) for 1 hour and ensured the membrane saturated with dyes. After that, the conventional separation process was performed using common-concentration organic dye feed (100 ppm). The resultant rejection values (R) were collected and compared with the origin rejection (R_0) value tested before. A R/R_0 ratio close to 1 means the adsorption of organic dyes doesn't greatly effect the rejection value.

Table S7. The summary of salt permeation of all the membranes tested in this work.

Membrane name	Na_2SO_4 permeation (%)	$MgSO_4$ permeation (%)	$MgCl_2$ permeation (%)
PAN substrate	100	100	100
POSS(0)/PDA(75)	86.5±0.2	98.8±0.1	99.0±0.1
POSS(5)/PDA(75)	86.9±0.2	98.9±0.1	99.2±0.1
POSS(8)/PDA(75)	87.5±0.2	99.0±0.1	99.0±0.2
POSS(10)/PDA(75)	88.9±0.1	99.0±0.2	99.1±0.1
POSS(12)/PDA(75)	90.0±0.1	99.0±0.1	99.1±0.1
POSS(16)/PDA(75)	90.2±0.1	99.0±0.1	99.1±0.1
POSS(12)/PDA(60)	93.7±0.1	99.5±0.1	99.5±0.1
POSS(12)/PDA(90)	89.6±0.2	98.9±0.1	98.9±0.2
POSS(12)/PDA(105)	87.8±0.2	98.8±0.2	98.8±0.2
POSS(12)/PDA(120)	86.9±0.2	98.5±0.2	98.6±0.2

Table S7 summarized the salt rejection of all the membranes tested in this work. (Testing condition: 1000 ppm salt feed under 0.1 MPa; 25 °C; 13.4 cm^2 membrane area; each above value was based on the average of two independent membranes fabricated under the same condition.)

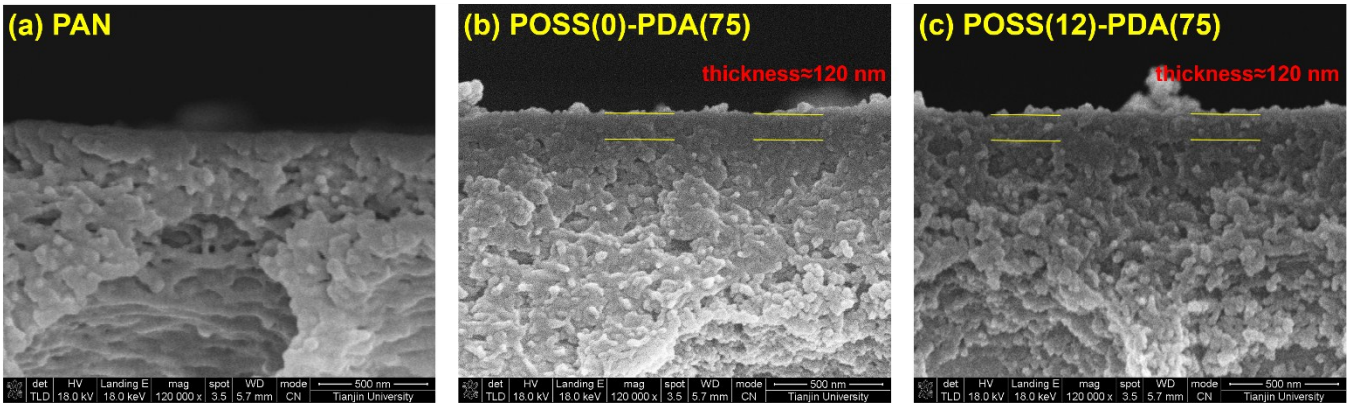

Fig. S11. The cross-section images of (a) PAN; (b) POSS(0)/PDA(75) and (c) POSS(12)/PDA(75).

Table S8. Comparison of the separation performance of different membranes in the literatures (in an order of permeance).

Membrane name	Permeance ($L\ m^{-2}\ h^{-1}\ MPa^{-1}$)	Dye rejection	Dye feed concentration (ppm)	Salt permeation	Salt feed concentration (ppm)	Selective factor (Na_2SO_4/dye)	Ref.
POSS-PDA/PAN	1099	90.5%, Orange GII	100	90%, Na_2SO_4	1000	9.5	this

		93.6%, Methyl blue		99%, $MgSO_4$		14.1	work
		98.0%, Congo red		99.1%, $MgCl_2$		45.0	
		93.9%, Alcian blue				14.8	
ZIF-8/PEI-HPAN	751	99.2%, Congo red 98.9%, Methyl blue	100	97%, NaCl	1000	-	2
F-PDA/PES	461	99%, Congo red	100	-	-	-	3
SiO_2-PIL-PES	375	90%, Reactive black 5	500	93.7%, NaCl	5000	-	4
TMC-GO	276	95%, Rhodamine-WT	7.5	74%, Na_2SO_4 81%, NaCl	1	14.8	5
Ra-PDA/PEI	262	98.1%, Reactive orange 16 99.4%, Direct red 23 >95%, Reactive blue 2 >80%, Rhodanile blue	500	94.9%, Na_2SO_4	1000	32.7 158 6.5 4.8	6
PEI-GA/PAN	255	97.1%, Congo red	100	95%, Na_2SO_4 87.5%, $MgSO_4$ 87.7%, $MgCl_2$ 89.9%, NaCl	1000	32.8	7
SiO_2-PSS-PES	233	>90%, Reactive black 5	500	87.2%, Na_2SO_4 77.5%, $MgSO_4$ 86.7%, $MgCl_2$ 94.9%, NaCl	-	8.7	8
brGO	218	99.2%, Methyl blue 99.9%, Direct red 81	0.4	70%, $MgSO_4$ 80%, $MgCl_2$ 42%, NaCl	33	-	1
Co-NF-2	~182	>90%, Reactive red 49 99.4%, Congo red 99%, Reactive blue 2	500	74.9%, Na_2SO_4 98.5%, $MgCl_2$ 97.3%, NaCl	1000	7.5 124.8 74.9	9
CS-MMT-PES	178	87.1%, Reactive black 5	500	81.2%, Na_2SO_4 78.3%, $MgSO_4$ 94.4%, $MgCl_2$ 93.9%, NaCl	-	6.3	10
Sepro NF 6	137	99.93%, Congo red	100	97.3%, NaCl	2500	-	11

		99.8%, Direct red 23					
QPEI-PES	127.5	~95%, Reactive black 5	500	83.7%, Na_2SO_4 85.5%, $MgSO_4$ 85.6%, $MgCl_2$ 92.5%, NaCl	-	16.7	12
GO-PSBMA/PES	~119.8	99.2%, Reactive black 5 97.2%, Reactive red 49	500	87.5%, Na_2SO_4 89.5%, $MgSO_4$ 91.8%, $MgCl_2$ 93.8%, NaCl	-	109.4 31.3	13
HNTs-PIL-PES	118	94-96%, Reactive black 5	-	95.5%, Na_2SO_4 91.5%, $MgSO_4$ 88.5%, $MgCl_2$ 92.7%, NaCl	-	19.1	14
CNT-GO	113	99%, Direct yellow 96%, Methyl orange	50	19%, Na_2SO_4 69.1%, $MgSO_4$ 90.4%, $MgCl_2$ 60.3%, NaCl	-	19 4.75	15
HBP/PAN	110	97%, Methyl blue	100	87.7%, NaCl	2000	-	16
TiO_2-GO	108	87.2%, Direct red	0.01	-	-	-	
Sepro NF 2A	105	99.96%, Congo red 99.95%, Direct red 23	100	77%, NaCl	330	-	11
mHT-PES	63	95%, Reactive black 5 90%, Reactive red 49	1000	93.4%, Na_2SO_4 86.3%, $MgSO_4$ 91.8%, $MgCl_2$ 88.8%, NaCl	-	18.7 9.3	17

References

1. Y. Han, Z. Xu and C. Gao, *Adv Funct Mater*, 2013, **23**, 3693-3700.
2. L. B. Yang, Z. Wang and J. L. Zhang, *J Mater Chem A*, 2017, **5**, 15342-15355.
3. Y. Li, Y. Su, X. Zhao, X. He, R. Zhang, J. Zhao, X. Fan and Z. Jiang, *Acs Appl Mater Inter*, 2014, **6**, 5548-5557.
4. L. Yu, Y. T. Zhang, Y. M. Wang, H. Q. Zhang and J. D. Liu, *Journal of Hazardous Materials*, 2015, **287**, 373-383.
5. M. Hu and B. Mi, *Environ Sci Technol*, 2013, **47**, 3715-3723.
6. J. Wang, J. Zhu, M. T. Tsehaye, J. Li, G. Dong, S. Yuan, X. Li, Y. Zhang, J. Liu and B. Van der Bruggen, *J. Mater. Chem. A*, 2017, **5**, 14847-14857.
7. S. Zhao and Z. Wang, *J Membrane Sci*, 2017, **524**, 214-224.
8. L. X. Xing, N. N. Guo, Y. T. Zhang, H. Q. Zhang and J. D. Liu, *Sep Purif Technol*, 2015, **146**, 50-59.

9. J. Y. Zhu, A. Uliana, J. Wang, S. S. Yuan, J. Li, M. M. Tian, K. Simoens, A. Volodin, J. Y. Lin, K. Bernaerts, Y. T. Zhang and B. Van der Bruggen, *J Mater Chem A*, 2016, **4**, 13211-13222.
10. J. Zhu, M. Tian, Y. Zhang, H. Zhang and J. Liu, *Chemical Engineering Journal*, 2015, **265**, 184-193.
11. J. Lin, W. Ye, H. Zeng, H. Yang, J. Shen, S. Darvishmanesh, P. Luis, A. Sotto and B. V. D. Bruggen, *J Membrane Sci*, 2015, **477**, 183-193.
12. J. Zhu, Y. Zhang, M. Tian and J. Liu, *Acs Sustainable Chemistry & Engineering*, 2015, **3**, 690-701.
13. J. Zhu, M. Tian, J. Hou, J. Wang, J. Lin, Y. Zhang, J. Liu and B. V. D. Bruggen, *J Mater Chem A*, 2015, **4**, 1980-1990.
14. L. Yu, Y. Zhang, H. Zhang and J. Liu, *Desalination*, 2015, **359**, 176-185.
15. Y. Han, Y. Jiang and C. Gao, *ACS Appl Mater Interfaces*, 2015, **7**, 8147-8155.
16. L. Wang, S. Ji, N. Wang, R. Zhang, G. Zhang and J. R. Li, *J Membrane Sci*, 2014, **452**, 143-151.
17. L. Yu, J. Deng, H. Wang, J. Liu and Y. Zhang, *Acs Sustainable Chemistry & Engineering*, 2016, **4**, 3292-3304.